

University of Groningen

Controlling molecular chirality and motion

van Delden, Richard Andreas

IMPORTANT NOTE: You are advised to consult the publisher's version (publisher's PDF) if you wish to cite from it. Please check the document version below.

Document Version

Publisher's PDF, also known as Version of record

Publication date:

2002

[Link to publication in University of Groningen/UMCG research database](#)

Citation for published version (APA):

van Delden, R. A. (2002). *Controlling molecular chirality and motion*. s.n.

Copyright

Other than for strictly personal use, it is not permitted to download or to forward/distribute the text or part of it without the consent of the author(s) and/or copyright holder(s), unless the work is under an open content license (like Creative Commons).

The publication may also be distributed here under the terms of Article 25fa of the Dutch Copyright Act, indicated by the "Taverne" license. More information can be found on the University of Groningen website: <https://www.rug.nl/library/open-access/self-archiving-pure/taverne-amendment>.

Take-down policy

If you believe that this document breaches copyright please contact us providing details, and we will remove access to the work immediately and investigate your claim.

Downloaded from the University of Groningen/UMCG research database (Pure): <http://www.rug.nl/research/portal>. For technical reasons the number of authors shown on this cover page is limited to 10 maximum.

Chapter 5

From Controlling Chirality to Controlling Rotation

*In this chapter the use of sterically overcrowded alkenes as unidirectionally rotating molecular motors is described. The work is an extension of the research on chiroptical molecular switches and the most important features will be treated in this context. The extension requires additional chiral information in the molecular structure to make the different forms of the sterically overcrowded alkene diastereomeric. Apart from an interesting pyrrolidine-functionalized donor-acceptor system, the first real example of a unidirectionally rotating motor is introduced.**

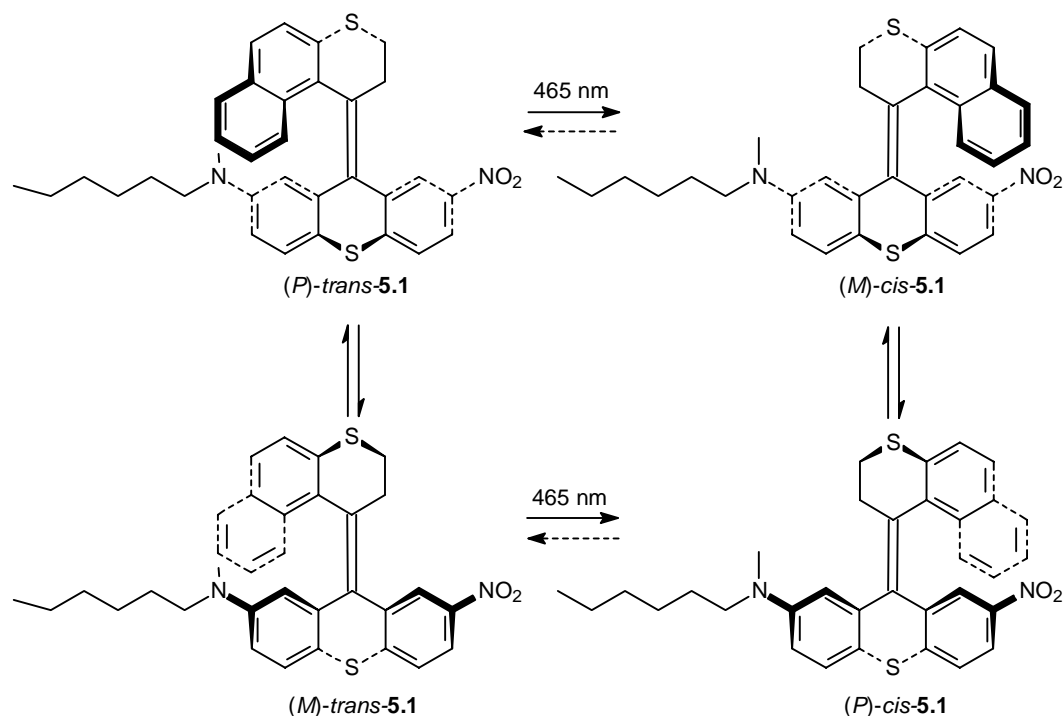
* Part of this chapter has been published: N. Koumura, R.W.J. Zijlstra, R.A. van Delden, N. Harada, B.L. Feringa, *Nature* **1999**, 401, 152.

5.1 Introduction

In the previous chapters it was shown that sterically overcrowded alkenes could function as chiroptical molecular switches. In these systems molecular chirality can be controlled by light. It was also demonstrated by employing liquid crystals as host compounds that macroscopic chirality could be controlled using chiroptical molecular switches as guest compounds. These systems might have potential in future nanotechnological applications such as optical data storage units or as true switching devices in optical data processing. Apart from these molecular switches which have one specific function, in approaches towards true nanoscale molecular devices a variety of different functions have to be addressed at the molecular level.¹ This requires delicate super- or supramolecular organization of different molecular components each capable of performing a certain function. A variety of molecular, mechanical type, components have been developed, including, next to molecular switches, molecular counterparts of brakes,² gears,³ turnstiles⁴ and muscles.⁵ A highly desirable addition to this so-called *toolbox of nanotechnology* is a molecular motor. In a molecular motor consumption of energy should result in controlled motion. This motion could eventually enable a device to perform mechanical work. If control of the direction of a full rotary motion in a molecular type motor can be realized, a basic requirement for the construction of (supra)molecular machines might be fulfilled. In Chapter 1 already some examples of molecular motors have been discussed. A chemically driven molecular motor that uses chemical energy to perform a 120° rotation has been developed by Kelly *et al.*⁶ Simultaneously, in our group a light-driven molecular motor based on a sterically overcrowded alkene was developed in which full 360° unidirectional rotation was accomplished. This chapter will elaborate on the step from molecular switching to molecular rotation for sterically overcrowded alkenes.

5.2 Extension of the Molecular Switching Movement

The chiroptical molecular switches already show a unidirectional rotation of about 105° as estimated from the X-ray structures discussed in Chapter 2. The direction of the movement is solely governed by the helicity in the initial state and the process is driven by light. In the development of molecular motors using sterically overcrowded alkenes as the basic structure, an extension of the switching movement is necessary and the light induced movement should continue in the same direction. Realizing that these sterically overcrowded alkenes consist of four stereoisomers, that is the pseudoenantiomeric forms that constitute the two switching stages and their enantiomers, the possibility of full 360° rotation arises. For the *n*-hexylmethylamino nitro donor-acceptor switch **5.1**, extensively discussed in the foregoing chapters, the possible processes are depicted in Scheme 5.1. Starting from enantiomerically pure (*P*)-*trans*-**5.1**, irradiation at 465 nm results in near quantitative formation of the (*M*)-*cis*-**5.1** isomer. Since the *cis*-isomer does not absorb light at this wavelength, this isomerization represents a unidirectional process.

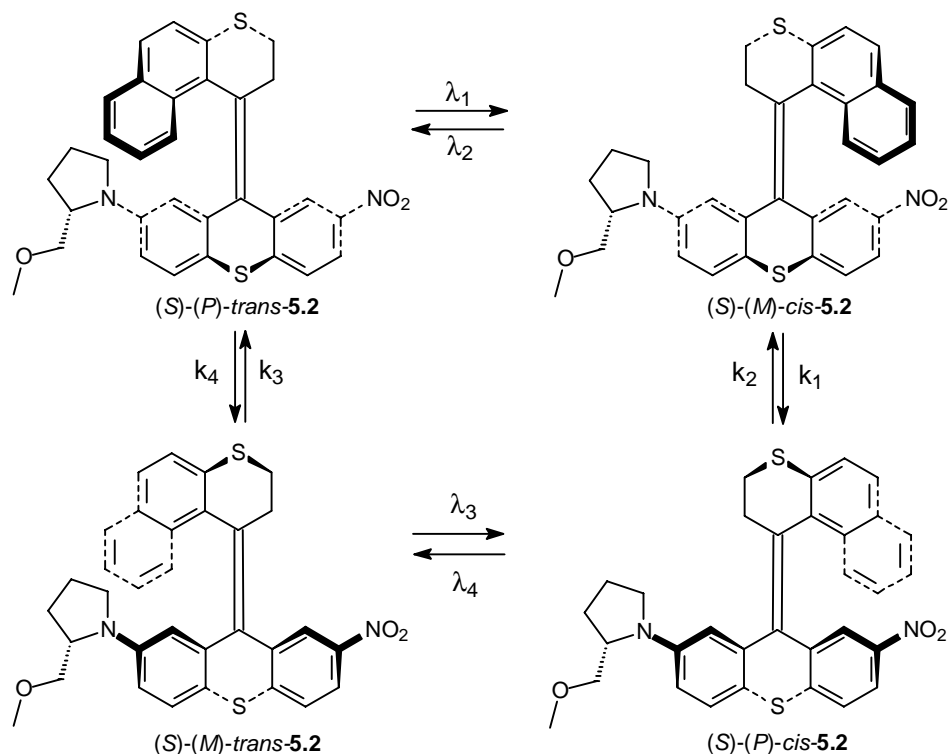


Scheme 5.1 Four states of a chiroptical molecular switch in theory combine to allow full rotation.

Racemization by heating the solution results in a helix inversion forming *(P)*-*cis*-**5.1** eventually leading to a racemic state. This combination of irradiation and heating results in a full 180° rotation from *(P)*-*trans*-**5.1** to *(P)*-*cis*-**5.1**, although an equal amount of *(M)*-*cis*-**5.1** will be present. Continuation of this movement for this system leads to a complicated mixture of all stereoisomers, as irradiation of the *cis*-isomers (*(M)*-*cis*-**5.1** and *(P)*-*cis*-**5.1**) at the most efficient wavelength (380 nm) will result in both *cis* to *trans* as well as *trans* to *cis* isomerization. This will eventually lead to a racemic mixture of *cis*- and *trans*-isomers in a 30 : 70 ratio, which was determined to be the photostationary state composition at this wavelength (Chapter 2). Theoretically it will never be possible to make a unidirectional molecular motor when two enantiomeric states of one single compound are involved in the process. Nevertheless, this short reasoning shows that the four stages of the molecular switch may combine to allow full rotary behavior. Although at specific wavelengths the photoequilibrium can efficiently be shifted to one side, as illustrated for compound **5.1**, *cis-trans* isomerization of the olefinic bond in these overcrowded alkenes is in principle reversible. Unidirectionality in rotation for a sterically overcrowded alkene should therefore be controlled in the thermal helix inversion steps, which for compound **5.1** are part of a racemization process. To achieve this unidirectionality an additional chiral influence is essential to differentiate between the forward helix inversion pathway and the reverse process.

5.3 Pyrrolidine Functionalized Chiroptical Molecular Switch

A possible candidate to function as a molecular motor is compound **5.2**. This sterically overcrowded alkene closely resembles the donor-acceptor substituted switch **5.1**. The intrinsically chiral structure is functionalized with an electron withdrawing nitro and an electron donating amine substituent. The amine in this case is the proline derivative (*S*)-2-methoxymethylpyrrolidine. This chiral amine has been used as a chiral auxiliary in asymmetric synthesis.⁷ The additional stereogenic center in this molecular switch results in four distinct diastereomeric forms, rather than two diastereomeric pairs of enantiomers as found for **5.1** (Scheme 5.2). As a result, the two photoequilibria are now different and also the helix inversion steps are no longer true racemizations but rather pseudoracemization processes. A difference in energy for the two separate *cis*- ((*S*)-(*M*)-*cis*-**5.2** / (*S*)-(*P*)-*cis*-**5.2**) and *trans*- ((*S*)-(*M*)-*trans*-**5.2** / (*S*)-(*P*)-*trans*-**5.2**) isomers of **5.2** can be anticipated. Due to the relatively large conformational freedom of the pyrrolidine moiety unfortunately no unequivocal data on this energy difference could be gained from computer calculations.



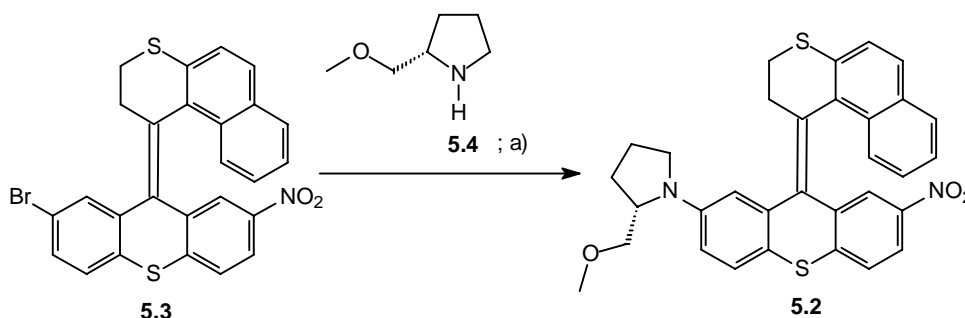
Scheme 5.2 Four diastereoisomers of chiroptical switch **5.2** and their transformations.

Next to the possible unidirectionality of the pseudoracemization steps, compound **5.2** offers some additional appealing features. The (*S*)-2-methoxymethylpyrrolidine substituent for example, might be suitable for attachment of the chiroptical switch to peptide chains after ether hydrolysis, which might be an important step towards switchable biomaterials.⁸ Another feature is that due to the diastereomeric relationship of all four forms of molecular switch **5.2**

chiral separation techniques are no longer essential in the resolution of these four stereoisomers.

5.3.1 Synthesis and Resolution

The synthesis of compound **5.2** was performed by J.H. Hurenkamp. A palladium-catalyzed amination of bromo-substituted switch **5.3** with (*S*)-2-methoxymethylpyrrolidine **5.4**, as discussed in detail in Chapter 2, was used. The (*S*)-2-methoxymethylpyrrolidine was synthesized according to a literature procedure starting from enantiomerically pure (*S*)-proline in a straightforward procedure with retention of chirality.⁷



Scheme 5.3 Functionalization reaction of bromo-substituted overcrowded alkene **5.3** to form **5.2** involving a palladium catalyzed amination: a) $\text{Pd}_2(\text{dba})_3$, BINAP, NaOtBu, toluene, 80°C, yield: 58%.

Chiroptical switch **5.2** was obtained as a mixture of the four diastereoisomers, as depicted in Scheme 5.2. Resolution was performed by HPLC over an achiral silica column. Using a gradient of *n*-heptane and dichloromethane as an eluent, the four diastereomers were readily separated with retention times of 16.9 min ((*S*)-(*M*)-*cis*-**5.2**); 17.4 min ((*S*)-(*P*)-*cis*-**5.2**); 18.2 min ((*S*)-(*P*)-*trans*-**5.2**); 18.8 min ((*S*)-(*M*)-*trans*-**5.2**). It should be noted again that for the chiroptical switches discussed in Chapter 2, time-consuming and expensive chiral resolution is necessary, whereas now achiral chromatography readily allows separation of the different isomers. The accessibility of the enantiomerically pure forms is an important advantage of compound **5.2** over all the other chiroptical switches discussed.

5.3.2 Switching Selectivity

Due to the diastereomeric relationship, the discussion on the switching selectivity of compound **5.2** is a little more complicated than for the other molecular switches. Since the two photoisomerizations here are no longer enantiomeric pathways they have to be analyzed separately. For the pseudoenantiomeric couple (*S*)-(*M*)-*cis*-**5.2** and (*S*)-(*P*)-*trans*-**5.2** (Scheme 5.4), UV-VIS and CD absorption curves were determined (Figure 5.1). The CD absorption curves indicate the respective (*P*)- and (*M*)-helicity with $\Delta\epsilon$ -values comparable to the other donor-acceptor switches (e.g. compound **5.1**). From the differences in the UV-VIS absorption, with values comparable to those of other donor-acceptor switches, the ideal wavelengths for switching could be determined. Here 380 nm and 463 nm were the most selective. Irradiation of an *n*-hexane solution of (*S*)-(*M*)-*cis*-**5.2** with 380 nm light resulted in a photostationary state consisting of (*S*)-(*P*)-*trans*-**5.2** and (*S*)-(*M*)-*cis*-**5.2** in a ratio of 69 : 31,

as determined by CD spectroscopy. Subsequent irradiation at 463 nm led to a photostationary state with excess (*S*)-(*M*)-*cis*-**5.2**. The diastereomeric ratio (*S*)-(*M*)-*cis*-**5.2** : (*S*)-(*P*)-*trans*-**5.2** was 96 : 4. This switching process was fully reversible. The selectivity of this switching process is as expected comparable to other donor-acceptor systems. The CD spectra of the photostationary states are also depicted in Figure 5.1. The absorption at longer wavelengths for the *trans*-isomer results in highly selective switching towards the *cis* photostationary state (irradiation at 463 nm), comparable to compound **5.1**.

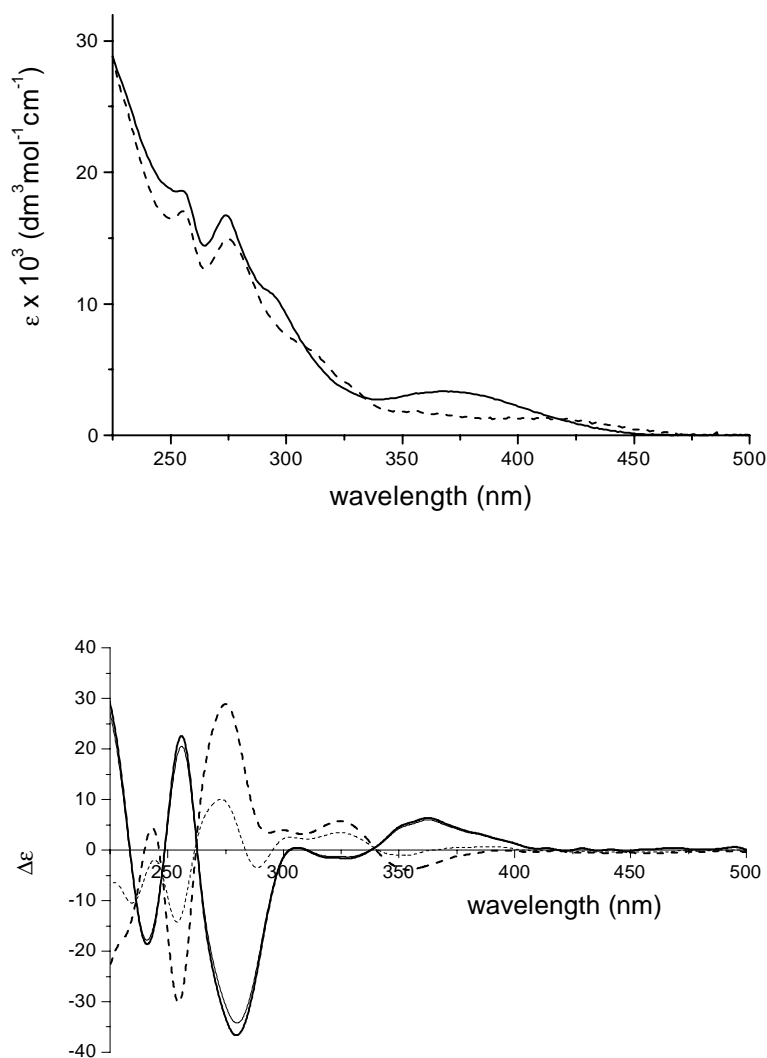
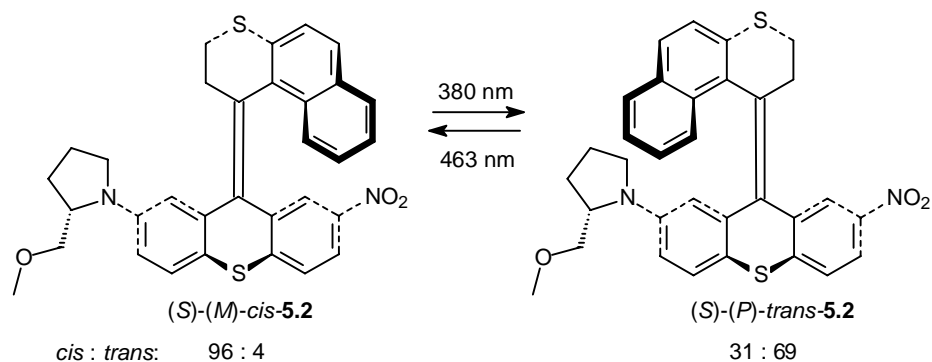
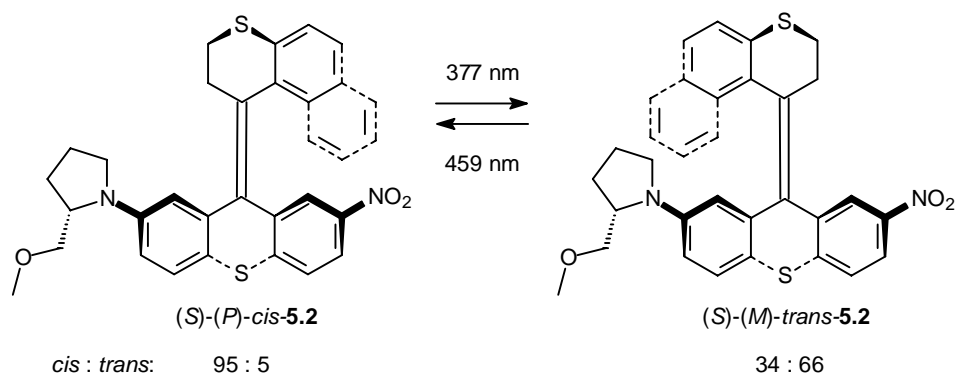


Figure 5.1 UV-VIS and CD absorption spectra of the diastereoisomers (*S*)-(*M*)-*cis*-**5.2** and (*S*)-(*P*)-*trans*-**5.2** in *n*-hexane. The solid curves correspond to (*S*)-(*M*)-*cis*-**5.2** and the dashed graphs to (*S*)-(*P*)-*trans*-**5.2**. The thin curves correspond to the photostationary states.



Scheme 5.4 Selective switching between two diastereoisomers $(S)-(M)\text{-}cis\text{-}5.2$ and $(S)-(P)\text{-}trans\text{-}5.2$.

In a completely analogous way, the UV-VIS and CD absorptions of the other pseudoenantiomeric couple: $(S)-(P)\text{-}cis\text{-}5.2$ and $(S)-(M)\text{-}trans\text{-}5.2$ were determined (Figure 5.2 and Scheme 5.5). The most efficient switching wavelengths here, again derived from the ratio of the two UV absorption curves, were 379 and 459 nm for the *trans* and the *cis* photostationary state, respectively. Irradiation at 379 nm resulted in a photostationary state consisting of $(S)-(M)\text{-}trans\text{-}5.2$ and $(S)-(P)\text{-}cis\text{-}5.2$ in a 66 : 34 ratio. Irradiation at 459 nm resulted in the formation of a *cis*-enriched photostationary state with a ratio of $(S)-(P)\text{-}cis\text{-}5.2$: $(S)-(M)\text{-}trans\text{-}5.2$ of 95 : 5. Hence, switching selectivities as well as UV-VIS and CD absorption characteristics are similar for the two diastereomeric bistable switching pairs. This is further illustrated in Figure 5.3 where both the UV-VIS as well as the CD absorption curves of the respective *cis*- and *trans*-isomers are directly compared.



Scheme 5.5 Selective switching between the other two diastereoisomers $(S)-(P)\text{-}cis\text{-}5.2$ and $(S)-(M)\text{-}trans\text{-}5.2$.

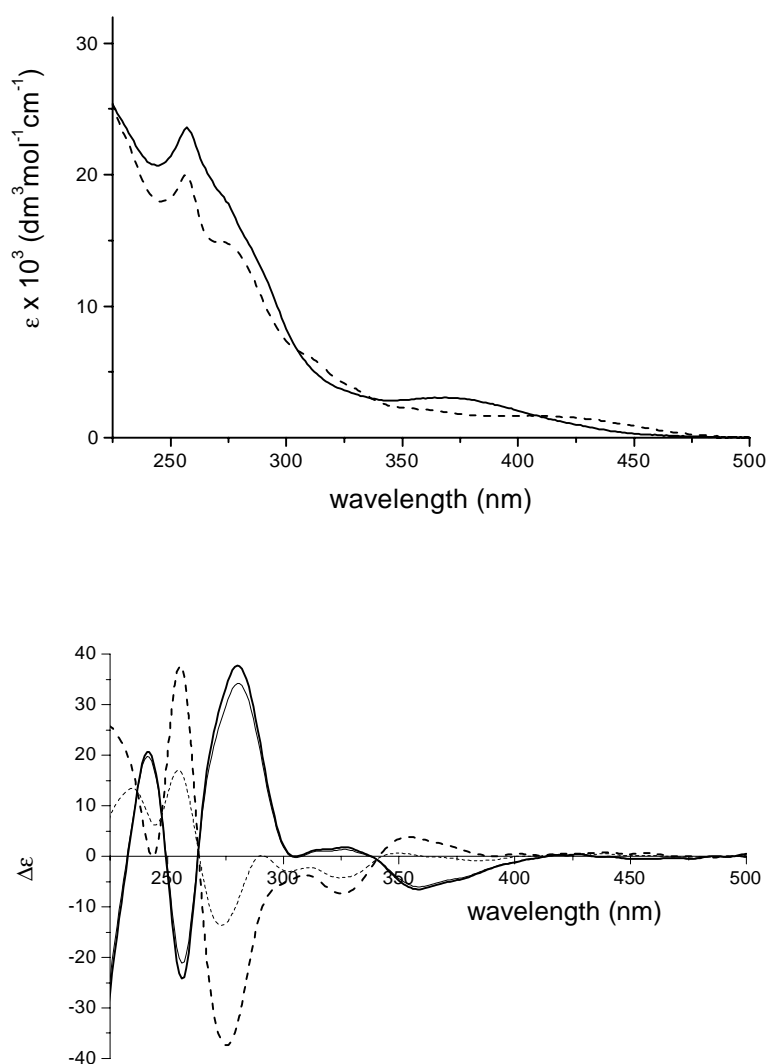


Figure 5.2 UV-VIS and CD absorption characteristics of the (S)-(P)-*cis*-**5.2** and (S)-(M)-*trans*-**5.2** diastereoisomers in *n*-hexane. The solid curves correspond to (S)-(P)-*cis*-**5.2** and the dashed graphs to (S)-(M)-*trans*-**5.2**. The thin curves correspond to the photostationary states.

Subtle differences in UV absorption result in the slightly different ideal switching wavelength as well as the slightly different switching selectivity. Only small differences in CD absorptions can be observed. The CD spectra of the *cis*- and *trans*-compounds of opposite helicity are, however, still roughly mirror images. The major differences are found in the UV absorption of the two isomers at lower wavelengths. These differences might be assigned to different geometries of the chiral amine-substituted aryl moiety absorbing in this region.

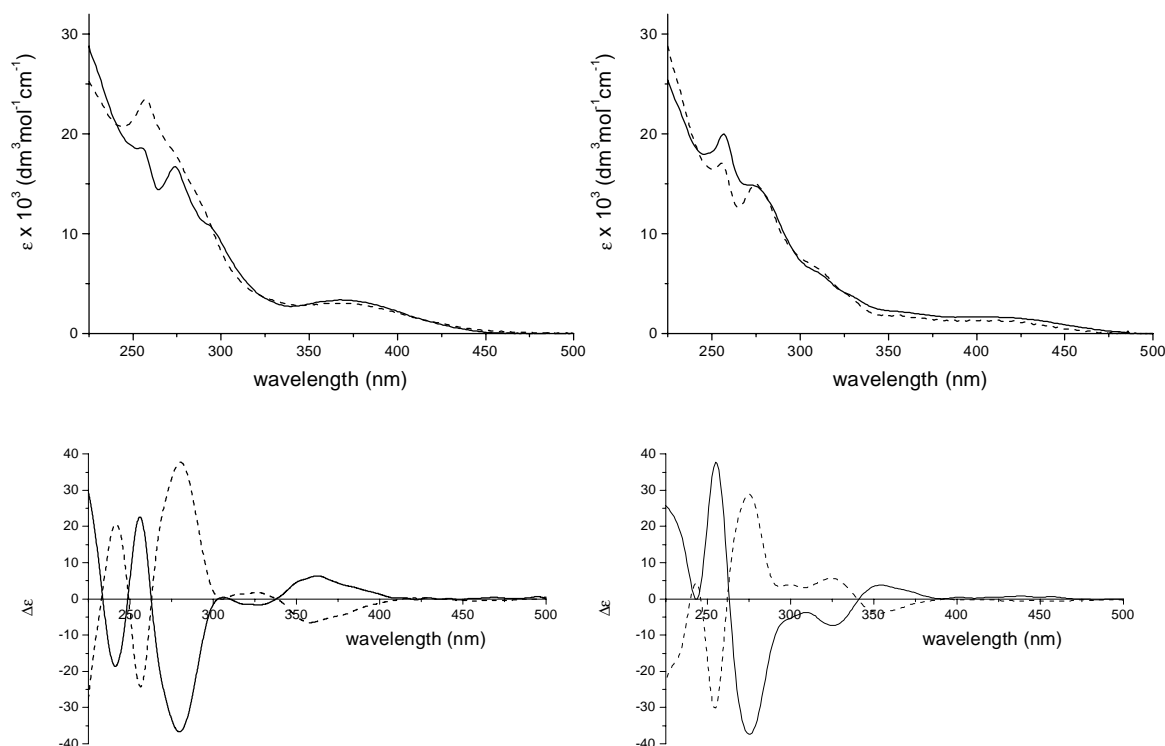


Figure 5.3 Comparison of UV-VIS and CD absorption characteristics of (*S*)-(*M*)-*cis*-**5.2** and (*S*)-(*P*)-*cis*-**5.2** (left) and (*S*)-(*M*)-*trans*-**5.2** and (*S*)-(*P*)-*trans*-**5.2** (right), respectively. Solid curves correspond to both the (*M*)-enantiomers; dashed curves correspond to both the (*P*)-enantiomers.

5.3.3 Thermal Stability of the Distinct Diastereoisomers

A small but significant effect of the additional stereogenic center in compound **5.2** was observed in the photophysical behavior of the four distinct diastereomers. A more important effect here, in the light of the development of molecular motors, is the influence of the additional stereogenic center on the thermal stability of the different stereoisomers. Where in the case of the donor-acceptor systems discussed in previous chapters, thermal stability was determined by monitoring the racemization at elevated temperatures, in the present system **5.2** one cannot speak of a true racemization. The thermally induced interconversion between the diastereoisomers (*S*)-(*M*)-*cis*-**5.2** and (*S*)-(*P*)-*cis*-**5.2**, and (*S*)-(*M*)-*trans*-**5.2** and (*S*)-(*P*)-*trans*-**5.2** was monitored in *n*-dodecane by CD spectroscopy. These pairs of diastereoisomers that share the same (*cis* or *trans*) configuration but show opposite helical shape might be called pseudoepimers.⁹ Solutions of enantiomerically pure (*S*)-(*M*)-*cis*-**5.2** and (*S*)-(*P*)-*trans*-**5.2** at known concentrations were heated for 10 h at 100°C. The change in CD absorption was monitored in time, as depicted in Figure 5.4.

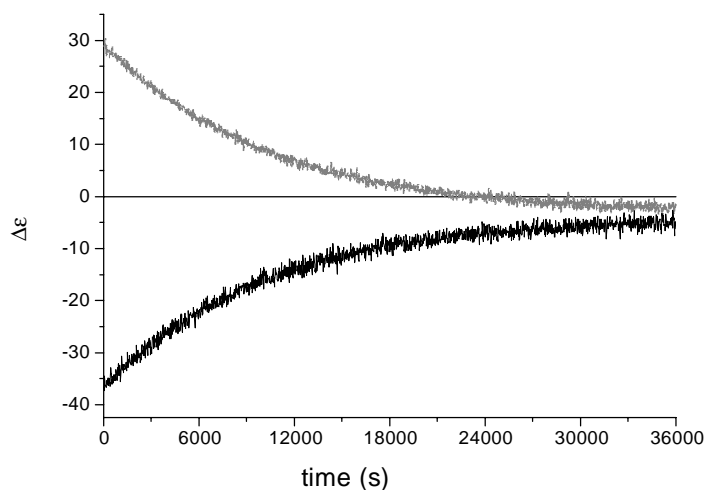
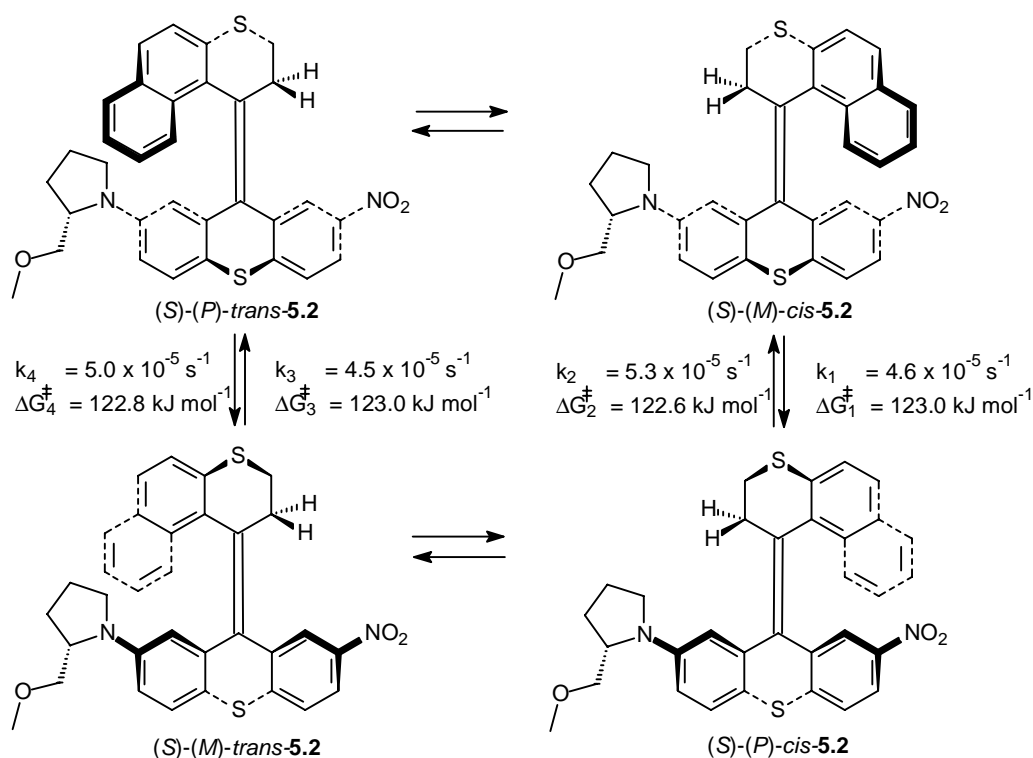


Figure 5.4 CD absorption rescaled to show molar values ($\Delta\epsilon$) in time for heated samples of (*S*)-(*M*)-*cis*-**5.2** (bottom) and (*S*)-(*P*)-*trans*-**5.2** (top) at 100°C in *n*-dodecane.

Knowing the molar CD absorption of all four diastereoisomers in this solvent, which are identical to the absorptions found in *n*-hexane, one can determine the equilibrium ratio of the two respective pseudoepimers. In case of (*S*)-(*M*)-*cis*-**5.2**, heating to equilibrium resulted in a steady state consisting of (*S*)-(*M*)-*cis*-**5.2** and (*S*)-(*P*)-*cis*-**5.2** in a 53.6 : 46.4 ratio. In case of the (*S*)-(*P*)-*trans*-**5.2** solution a steady state of (*S*)-(*P*)-*trans*-**5.2** and (*S*)-(*M*)-*trans*-**5.2** in a ratio of 47.5 : 52.5 was obtained. These steady state ratios are not 50 : 50 indicating that there is indeed a small but significant energy difference between the two *cis*- and the two *trans*-forms of **5.2**. These equilibrium ratios combined with the actual rate of the pseudoracemizations observed give the rate constants of all four separate pathways.¹⁰ From these *k*-values, the Gibbs energy of activation of the four distinct pathways, which is an indication for the relative stability of the four isomers, can be determined. The calculated values are depicted in Scheme 5.6.

Although the additional stereogenic center clearly has an effect on the relative stability of the distinct isomers the effects are very small. It should be noted that both for the *trans* as well as the *cis*-isomers (*M*)-helicity is preferred, however, no explanation for this behavior can be given at this moment. It might seem unexpected that the energy difference between the two *trans*-nitro isomers is in fact smaller than the difference for the two *cis*-nitro isomers. At first inspection of the molecule it would seem that the influence of the stereogenic center of the pyrrolidine substituent, which is solely responsible for the observed energy differences, is larger when it is in close proximity to the sterically demanding upper arene part of the molecule. It was, however, previously observed that in these complicated helical structures the two hydrogens directly adjacent to the central double bond in the upper half of the molecule (explicitly depicted in Scheme 5.6) have a more substantial steric effect on the lower half as discussed in Chapter 1 for molecular rotor **1.19**.¹¹ Where the two hydrogens are restricted to their respective axial and equatorial orientation, the naphthalene molecule can

simply bend away thereby greatly reducing the steric effect exerted on the lower half of the molecule.



Scheme 5.6 Thermal stabilities for the four distinct diastereoisomers of **5.2**.

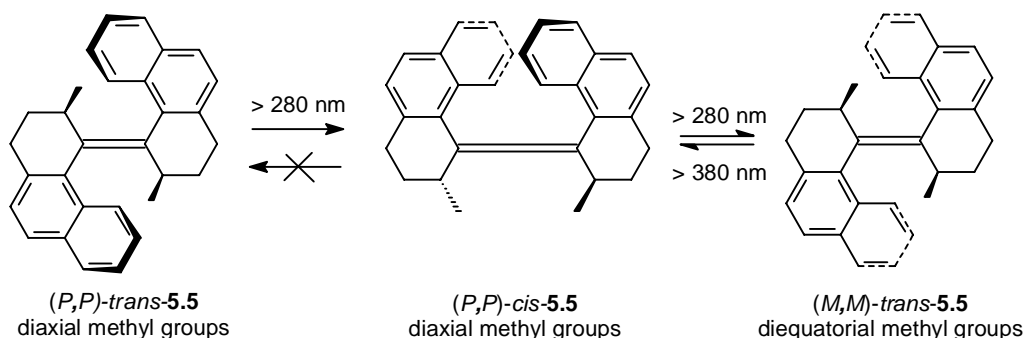
Although the energy differences shown in Scheme 5.6 are too small for any control on the directionality in these pseudoracemization processes, compound **5.2** has some advantageous properties compared to previously discussed donor-acceptor switches. The improved resolution properties of the system in combination with a high switching selectivity make this compound a potentially useful member of the chiroptical molecular switch family. The system will, however, never function as a molecular motor. Based on the same principle of chiral discrimination induced by an additional stereocenter in a sterically overcrowded alkene a molecular motor was however developed. A sterically overcrowded biphenanthrylidene bearing two stereocenters was proven to function as the first light-driven unidirectional molecular motor.

5.4 A Biphenanthrylidene as a Molecular Motor

The dimethyl-substituted biphenanthrylidene **5.5** is a sterically overcrowded alkene bearing two additional stereogenic centers. These biphenanthrylidenes,¹² both with respect to their photochemistry as well as their chiral features, closely resemble the sterically overcrowded alkenes used as chiroptical switches. Extensive research on these overcrowded alkenes has been performed in our group in collaboration with the group of professor Harada.¹³ These systems, like the molecular switches, due to the steric hindrance around the central double bond adopt a helical geometry. For full assignment of the helices in this case both halves of

the molecule have to be designated separately leading to (*M,M*)-, (*P,P*)- and (*M,P*)-isomers. For the unsubstituted biphenanthrylidenes already remarkable racemization behavior was observed where the *cis*-isomers were shown to racemize considerably faster than the *trans*-isomers.^{13b} For the methyl-substituted compound (*3R,3'R*)-1,1',2,2',3,3',4,4'-octahydro-3,3'-dimethyl-4,4'-biphenanthrylidene **5.5** both stereogenic centers are of (*R*)-configuration.¹⁴ The (*P,P*)-*trans*-isomer was found to be the most stable form due to the *trans*-geometry and the preferred axial orientation of both the methyl substituents. A chiral resolution and also a stereoselective synthesis for these types of systems has been reported.¹⁵

Photoisomerization (> 280 nm) of the stable (*P,P*)-*trans*-isomer at room temperature in solution unexpectedly resulted in the irreversible formation of the (*P,P*)-*cis*-isomer, which is also energetically stable due to the axial orientation of the two methyl substituents (Scheme 5.7).¹⁶ Although *trans*-*cis* isomerization occurred, the helicity of the *cis* state formed was the same as for the initial *trans*-state and the isomerization process was irreversible, both observations are in sharp contrast with our experience with other sterically overcrowded alkenes. A similar photoisomerization of the (*P,P*)-*cis*-isomer, using the same wavelength of light resulted in a reversible process to form the anticipated (*M,M*)-*trans*-isomer. The photostationary state consists of (*P,P*)-*cis*-**5.5** : (*M,M*)-*trans*-**5.5** in a ratio of 10 : 90. This (*M,M*)-*trans*-isomer is energetically less stable, by 36.0 kJ mol⁻¹ compared to the (*P,P*)-*trans*-isomer, due to the forced equatorial orientations of the methyl groups. It was found (by NMR analysis) to revert to the more stable (*P,P*)-*trans*-isomer in a unidirectional helix inversion step upon heating.



Scheme 5.7 Unexpected photochemistry of dimethyl-substituted biphenanthrylidene **5.5**.

Close examination of the processes using MOPAC93-AM1 calculations¹⁷ revealed that the reason for the unexpected formation of (*P,P*)-*cis*-**5.5** directly by photoisomerization of (*P,P*)-*trans*-**5.5** most probably would be the existence of an energetically highly unfavorable intermediate. This intermediate would be less stable by 46.0 kJ mol⁻¹ compared to the stable (*P,P*)-*cis*-isomer. It was proposed that this would be the expected (*M,M*)-*cis*-isomer of **5.5**. Low temperature (-50°C) UV-VIS experiments during irradiation of (*P,P*)-*trans*-**5.5** indeed revealed the formation of a fourth form of this system (Figure 5.5). The UV-VIS absorptions were bathochromically shifted and as a result the solution turned from colorless to yellow. Upon increase of the temperature to room temperature again the previously observed colorless (*P,P*)-*cis*-isomer of **5.5** was formed.

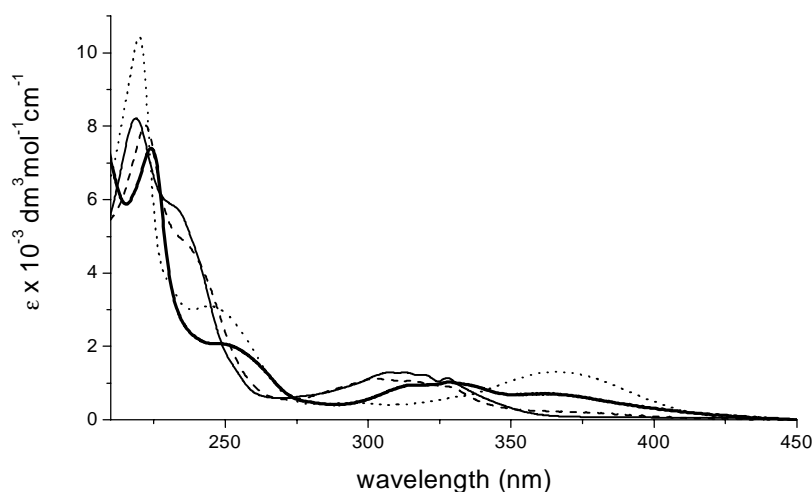


Figure 5.5 UV-VIS spectra (*n*-hexane) of the three forms of motor **5.5** stable at room temperature (thin solid: *(P,P)*-*trans*-**5.5**; dashed: *(P,P)*-*cis*-**5.5**; dotted: *(M,M)*-*trans*-**5.5**) and the UV spectrum obtained from low temperature irradiation of *(P,P)*-*trans*-**5.5**: thick black.

Detailed low temperature irradiation experiments combined with CD and NMR studies performed in a joint effort with N. Koumura in our group fully established that this fourth state was indeed the anticipated *(M,M)*-*cis*-isomer. A photostationary state consisting of *(P,P)*-*trans*-**5.5** : *(M,M)*-*cis*-**5.5** in a ratio of 5 : 95 was formed (at -50°C). The CD spectra of the four forms are depicted in Figure 5.6. The CD spectrum of *(M,M)*-*cis*-**5.5** is most illustrative for the chiral configuration since the Cotton effects are indicative of the *(M,M)*-helicity.

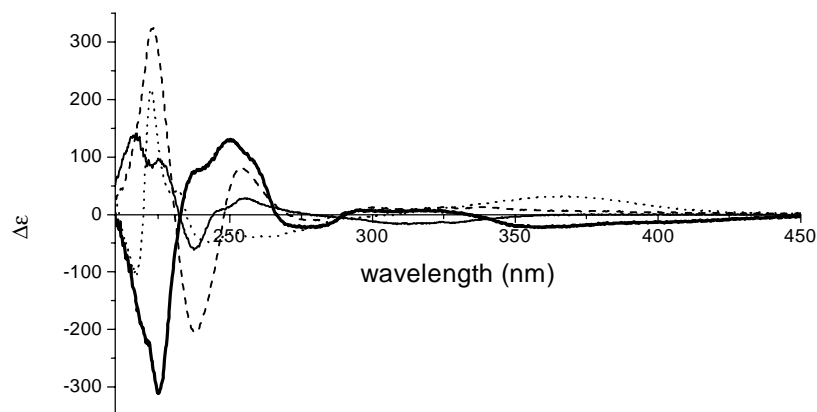
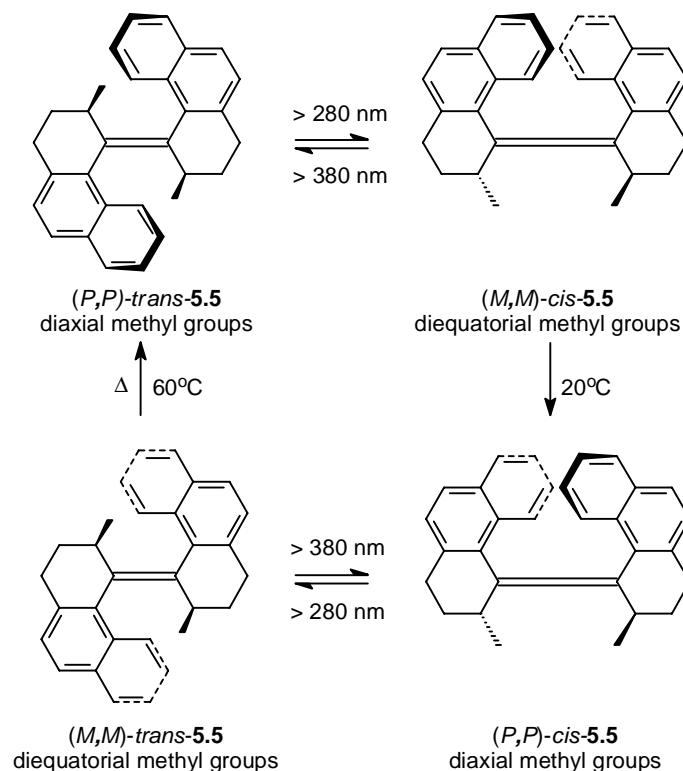


Figure 5.6 CD spectra (*n*-hexane) of the four forms of motor **5.5** (thin solid: *(P,P)*-*trans*-**5.5**; thick solid: *(M,M)*-*cis*-**5.5**; dashed: *(P,P)*-*cis*-**5.5**; dotted: *(M,M)*-*trans*-**5.5**) at -50°C.

The photoisomerization steps show remarkably high selectivity in switching to the *cis*-state, especially when we compare this hydrocarbon not containing any hetero-atom with the asymmetrically-substituted donor-acceptor switches such as **5.1** and **5.2** (*vide supra*). This is probably due to a quantum yield effect in going to the state with equatorial methyl groups which is the case for both photoisomerization processes (*P,P*)-**trans-5.5** to (*M,M*)-**cis-5.5** and (*P,P*)-**cis-5.5** to (*M,M*)-**trans-5.5**. It appears that the small differences in absorption (Figure 5.5) can never account for this high selectivity. All the data together combine to a four state switch where all the states can separately be addressed using combined irradiation and heating or cooling (Scheme 5.8).



Scheme 5.8 Four state molecular switch combining to unidirectional rotation.

Closer examination of the combined process reveals that the four discrete steps add up to a full 360° unidirectional rotation. Two photochemical energetically *uphill trans-cis* isomerizations, driving the rotary movement, are each followed by two irreversible energetically *downhill* thermal helix inversions, (*M,M*)-**cis-5.5** to (*P,P*)-**cis-5.5** and (*M,M*)-**trans-5.5** to (*P,P*)-**trans-5.5**. The first thermal isomerization occurs readily at room temperature. The second helix inversion is induced by heating the system to 60°C. The release of internal energy of the system that takes place during helix inversion, to place the methyl substituents again in the more favorable axial orientation, ensures the unidirectionality of the process. The direction of rotation is solely governed by the configuration of the stereogenic centers since this determines the axial or equatorial orientation of the methyl groups. Essential features of the rotating system are the olefinic bond, the helicity of the overcrowded alkene, the absolute configuration of the stereogenic centers and the conformational flexibility of the cyclohexyl-like rings. Due to the same wavelength used for

both the photoisomerizations of (*P,P*)-*trans*-**5.5** to (*M,M*)-*cis*-**5.5** and of (*P,P*)-*cis*-**5.5** to (*M,M*)-*trans*-**5.5**, a continuous unidirectional rotation can be induced by continuous irradiation at elevated temperature (above 60°C). As such this is the first example of a light-driven unidirectional molecular motor as illustrated in Figure 5.7. It should be noted here that this continuous rotation is not constant in speed, since the thermal and photoisomerization steps are discrete processes.

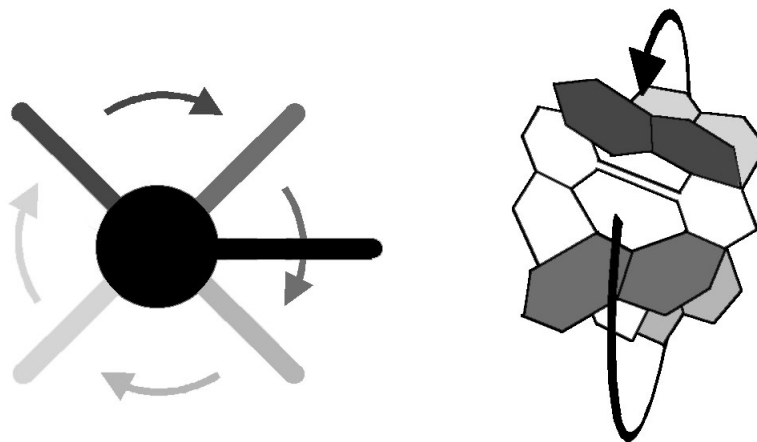


Figure 5.7 Continuous unidirectionally rotating molecular motor.

As already noted for the chiroptical molecular switches, for future application of these unidirectionally rotating systems, preservation of the molecular properties in an organized medium is absolutely essential.¹⁸ Furthermore the unique dynamic (chiral) properties of the rotating molecular system might allow photo-induced rotation to have an effect on macroscopic properties. Studies on polymer systems employing molecular motors and molecular motors assembled on a surface are already underway in our group. The research presented in the next chapter is focussing on liquid crystals as a host material because of the ability to amplify molecular chirality together with the advantage of processability of a liquid crystalline matrix as was discussed in Chapter 3 for the chiroptical molecular switches.

5.5 Conclusion

The step from molecular switches to molecular motors, based on sterically overcrowded alkenes requires an extension of the *cis-trans* isomerization process to full rotation around the central olefinic bond. The combination of isomerization and racemization in case of the chiroptical molecular switches allows for such a full rotation, but the direction of rotation is not controlled. Controlled rotation in these systems requires controlled unidirectional helix inversion rather than bidirectional racemization. The presence of a second chiral entity is essential. For pyrrolidine-substituted donor-acceptor switch **5.2**, a pending stereogenic center resulted in four different diastereoisomers. The differences between these diastereoisomers, however, were too small to allow unidirectional rotation even to some extent. Tiny energy differences were observed for the different *cis*- and *trans*-isomers of **5.2**. The additional stereogenic center compared to related donor-acceptor substituted switches, however, had a

large effect on the resolution of the different forms of this molecular switch. Due to their diastereomeric relationship all four possible structures were readily separated by achiral chromatographic techniques. Compound **5.2** proved to be a highly selective switch, comparable to other donor-acceptor systems developed earlier.

Unidirectional rotary behavior was found for the dimethyl-substituted biphenanthrylidene **5.5**. This is the first example of a light-driven molecular motor although almost simultaneously a chemically driven (120°) unidirectional molecular rotation was described for a tryptcene based molecular motor (see discussion in Chapter 1).⁶ The full 360° rotation with motor **5.5** is solely governed by the configuration around two stereogenic centers in the molecule. The stereochemical control is dramatically larger than that for compound **5.2** due to fact that the stereogenic center is part of the ring system in this sterically overcrowded alkene. The large energy differences between an axial and an equatorial orientation of the methyl substituents directly adjacent to the stereogenic centers results in highly efficient unidirectional rotation. These results illustrate the delicate influences of chirality in these sterically overcrowded systems. The properties of this molecular motor in liquid crystalline phases will be the subject of the next chapter. In Chapter 7 a different type of molecular motor is described which is actually a combination of the two systems discussed in this chapter.

5.6 Experimental Section

For general remarks, details of photochemical experiments and photophysical measurements see Section 2.6. The synthesis of bromo-substituted alkene **5.3** was described in Chapter 2. The synthesis, resolution and photochemical and thermal isomerization of **5.5** described elsewhere.^{13,19}

(S)-2-methoxymethylpyrrolidine 5.4.⁷ Under exclusion of oxygen, LiAlH_4 (14 g, 0.4 mol) and anhydrous THF (600 ml) were heated to reflux for 15 min. The heating mantle was switched off, (*S*)-proline (25 g, 0.25 mol) was added in small portions and the mixture was heated for 1 h at reflux. Excess LiAlH_4 was decomposed by cautiously adding a solution of KOH (7 g) in H_2O (28 ml). After stirring for 15 min the mixture was filtered through a large Büchner funnel and the remaining salts were extracted with THF (200 ml) using soxlet apparatus. The combined organic filtrates were concentrated under reduced pressure at 30°C . Methyl formate (18 ml, 17 g, 0.28 mol) was added at 0°C over a period of 1 h to the crude product and the mixture was stirred for 2 h. Excess methyl formate was evaporated at 30°C *in vacuo* affording a dark oil which was taken up in CH_2Cl_2 (150 ml) and dried with Na_2SO_4 . The mixture was filtered and concentrated under reduced pressure at 30°C . The procedure yielded 28.3 g (ca. 0.22 mol) of the crude N-formyl compound which was dissolved in anhydrous THF (350 ml). The solution was cooled to -60°C and MeI (18 ml, 0.26 mol) and then NaH (6.26 g, 0.26 mol) were added carefully. The solution was allowed to warm up to r.t. (H_2 gas evolves), heated to reflux for 15 min, quenched by slow addition of 6 M HCl (20 ml) and filtered. THF was evaporated under reduced pressure yielding a dark oil. A solution of KOH (40 g) in H_2O (156 ml) was added to the crude product under vigorous stirring at r.t. and the mixture was heated at reflux for 5 h. (*S*)-2-Methoxymethylpyrrolidine was extracted in a 500 ml perforator over a period of 24 h with diethylether. The organic layer was dried using Na_2SO_4 , diethylether was evaporated and product purified using bulb to bulb distillation (bp. $62^\circ\text{C}/40\text{Torr}$). The procedure yielded 10.56 g (37% overall

yield) of **5.4** as a colorless liquid which was stored at -4°C . ^1H NMR: δ 1.23-1.30 (m, 1H), 1.56-1.72 (m, 3H), 2.44 (s, 1H), 2.71-2.87 (m, 2H), 3.11-3.21 (s, 3H); ^{13}C NMR: δ 23.72(t), 26.27(t), 44.82(t), 56.11(q), 57.36(d), 74.58(t).

7-((S)-2-methoxymethylpyrrolidine)-2-nitro-9-(1',2',3',4'-tetrahydrophenanthrene-4'yldene)-9H-thioxanthene 5.2. BINAP (15 mg, 0.0225 mmol) and $\text{Pd}_2(\text{DBA})_3$ (7.5 mg, 0.0063 mmol) were dissolved in dry toluene (50 ml). This solution was stirred for half an hour at r.t. whereupon it turned from dark red to dark orange. After this period NaOt-Bu (125 mg, 1.3 mmol) was added, followed by bromo-substituted alkene **5.3** (100 mg, 0.19 mmol) and (S)-2-methoxymethylpyrrolidine **5.4** (50 mg, 0.43 mmol). The mixture was stirred at 80°C for 2 d. After this period the reaction mixture was poured into CH_2Cl_2 (50 ml) and filtered. The solvents were evaporated. The crude product was dissolved in a small amount of CH_2Cl_2 and purified using column chromatography (SiO_2 ; CH_2Cl_2 : *n*-hexane : NEt_3 50 : 50 : 1) to afford **5.2** as a red solid (60 mg, 58%). MS (EI): 552 [M+].

Resolution was performed by HPLC over an achiral silica column (Econosphere Silica; $5\ \mu\text{m}$; $250 \times 4.6\ \text{mm}$). The following gradient of *n*-heptane and dichloromethane was used as an eluent: 0-3 min pure *n*-heptane; 3-15 min gradient *n*-heptane : dichloromethane 100 : 0 to 0 : 100; 15-20 min pure dichloromethane; 20-21 min gradient *n*-heptane : dichloromethane 0 : 100 to 100 : 0. The four diastereomers are readily separated with retention times of 16.9 min ((S)-(M)-*cis*-**5.2**); 17.4 min ((S)-(P)-*cis*-**5.2**); 18.2 min ((S)-(P)-*trans*-**5.2**); 18.8 min ((S)-(M)-*trans*-**5.2**).

^1H NMR : (S)-(M)-*cis*-**5.2** and (S)-(P)-*cis*-**5.2**: δ 1.92-2.06 (m, 8H), 2.24-2.31 (m, 2H), 3.08-3.26 (m, 4H), 3.34 (s, 3H), 3.38 (s, 3H), 3.43-3.58 (m, 8H), 3.76-3.88 (m, 3H), 3.90-3.98 (m, 1H), 6.59 (t, $J = 2.2\ \text{Hz}$, 1H), 6.62 (t, $J = 2.2\ \text{Hz}$, 1H), 6.87 (t, $J = 2.6\ \text{Hz}$, 2H), 6.91-6.96 7.01-7.06 (m, 2H), 7.18-7.24 (m, 2H), 7.28-7.59 (m, 14H); (S)-(M)-*trans*-**5.2** and (S)-(P)-*trans*-**5.2**: δ 1.92-2.06 (m, 8H), 2.24-2.31 (m, 2H), 3.08-3.26 (m, 4H), 3.17 (s, 3H), 3.21 (s, 3H), 3.43-3.58 (m, 8H), 3.76-3.88 (m, 3H), 3.90-3.98 (m, 1H), 5.77 (d, $J = 2.2\ \text{Hz}$, 1H), 5.87 (d, $J = 2.2\ \text{Hz}$, 1H), 6.08 (dd, $J = 8.4, 2.2\ \text{Hz}$, 1H), 6.14 (dd, $J = 8.4, 2.2\ \text{Hz}$, 1H), 7.01-7.16 (m, 6H), 7.47-7.60 (m, 8H), 7.67 (d, $J = 8.4\ \text{Hz}$, 2H), 8.07-8.13 (m, 2H), 8.34 (d, $J = 2.2\ \text{Hz}$, 1H), 8.39 (d, $J = 2.2\ \text{Hz}$, 1H).

(S)-(M)-*cis*-**5.2** UV (*n*-hexane): λ_{max} (ϵ) 255 (18610), 273 (16686), 368 (3385); CD (*n*-hexane): λ_{max} ($\Delta\epsilon$) 241 (-18.6), 256 (+22.6), 280 (-36.7), 326 (-1.6), 362 (+6.3). (S)-(P)-*cis*-**5.2** UV (*n*-hexane): λ_{max} (ϵ) 257 (23552), 287 (13652), 369 (3058); CD (*n*-hexane): λ_{max} ($\Delta\epsilon$) 241 (+20.7), 255 (-24.2), 280 (-37.7), 326 (+1.8), 358 (-6.5). (S)-(M)-*trans*-**5.2**: UV (*n*-hexane): λ_{max} (ϵ) 257 (20005), 271 (14895), 312 (5942), 355 (2229), 398 (1681); CD (*n*-hexane): λ_{max} ($\Delta\epsilon$) 243 (0), 255 (+37.7), 275 (-37.4), 325 (-7.3), 353 (+3.8). (S)-(P)-*trans*-**5.2**: UV (*n*-hexane): λ_{max} (ϵ) 255 (17065), 275 (14981), 312 (6287), 327 (3882), 362 (1618), 402 (1681); CD (*n*-hexane): λ_{max} ($\Delta\epsilon$) 242 (+4.4), 255 (-30.3), 275 (+28.9), 325 (+5.7), 354 (-3.9).

5.7 References and Notes

- a) Sci Amer. Special Issue: *Nanotech: the science of small gets down to business*, September **2001**.
 - b) R.P. Feynman in *Miniturization*; H.D. Gilbert Ed.; Reinhold; New York, **1971**; c) K.E Drexler, *Nanosystems: Molecular Machinery, Manufacturing and Computation*; Wiley; New York, **1992**.
 - d) R.D. Astumian, *Sci. Amer.* July **2001**, 45.
- T.R. Kelly, M.C. Bowyer, *J. Am. Chem. Soc.* **1994**, 116, 3657.

- ³ a) A.M. Stevens, C.J. Richards, *Tetrahedron Lett.* **1997**, 38, 7805. b) J. Clayden, J.H. Pink, *Angew. Chem. Int. Ed. Engl.* **1998**, 37, 1937.
- ⁴ T.C. Bedard, J.S. Moore, *J. Am. Chem. Soc.* **1995**, 117, 10662.
- ⁵ M.C. Jiménez, C. Dietrich-Buchecker, J.-P. Sauvage, *Angew. Chem. Int. Ed.* **2000**, 39, 3284.
- ⁶ a) T.R. Kelly, H. de Silva, R.A. Silva, *Nature* **1999**, 401, 150; b) T.R. Kelly, R.A. Silva, H. de Silva, S. Jasmin, Y. Zhao, *J. Am. Chem. Soc.* **2000**, 122, 6935; c) T.R. Kelly, *Acc. Chem. Res.* **2001**, 34, 514.
- ⁷ D. Enders; M. Klatt, *Synthesis* **1996**, 12, 1403.
- ⁸ For an extensive account on biomolecular switches, see: I. Willner, B. Willner in *Chiroptical Molecular Switches*, B.L. Feringa Ed., Wiley-VCH, Weinheim, **2001**, Chapter 6, pp. 165-218.
- ⁹ Based on the term pseudoenantiomers; for stereochemical definitions see: E.L. Eliel, S.H. Wilen, *Stereochemistry of Organic Compounds*, Wiley, New York, **1994**.
- ¹⁰ The measured rate constant k for the process is a sum of the two individual rate constants of the reversible helix inversion, for *cis*-**5.2**: (*M*)-*cis*-**5.2** \rightarrow (*P*)-*cis*-**5.2** rate: k_1 ; (*P*)-*cis*-**5.2** \rightarrow (*M*)-*cis*-**5.2** rate k_2 then $k_{\text{measured}} = k_1 + k_2$. The ratio of the two components at equilibrium $[(M)\text{-}cis\text{-}5.2]/[(P)\text{-}cis\text{-}5.2] = K = k_2 / k_1$ was determined separately resulting in two equations with two unknown parameters that can be solved. For a unimolecular reaction: $\Delta G^\ddagger = -RT \ln (k_h / k_b T)$.
- ¹¹ A.M. Schoevaars, W. Kruizinga, R.W.J. Zijlstra, N. Veldman, A.L. Spek, B.L. Feringa, *J. Org. Chem.* **1997**, 62, 4943.
- ¹² B.L. Feringa, H. Wynberg, *J. Am. Chem. Soc.* **1977**, 99, 602.
- ¹³ a) N. Harada, A. Saito, N. Koumura, H. Uda, B. de Lange, W.F. Jager, H. Wynberg, B.L. Feringa, *J. Am. Chem. Soc.* **1997**, 119, 7241; b) N. Harada, A. Saito, N. Koumura, D.C. Roe, W.F. Jager, R.W.J. Zijlstra, B. de Lange, B.L. Feringa, *J. Am. Chem. Soc.* **1997**, 119, 7249; c) N. Harada, N. Koumura, B.L. Feringa, *J. Am. Chem. Soc.* **1997**, 119, 7256; d) R.W.J. Zijlstra, W.F. Jager, B. de Lange, P.T. van Duijnen, B.L. Feringa, H. Goto, A. Saito, N. Koumura, N. Harada, *J. Org. Chem.* **1999**, 64, 1667.
- ¹⁴ N. Koumura, N. Harada, *Enantiomer* **1998**, 3, 251
- ¹⁵ a) M.K.J. Ter Wiel, N. Koumura, R.A. van Delden, A. Meetsma, N. Harada, B.L. Feringa, *Chirality* **2000**, 12, 734; b) M.K.J. ter Wiel, N. Koumura, R.A. van Delden, A. Meetsma, N. Harada, B.L. Feringa, *Chirality* **2001**, 13, 336.
- ¹⁶ N. Koumura, N. Harada, *Chem. Lett.* **1998**, 1151.
- ¹⁷ Calculation performed by Dr. R.W.J. Zijlstra using MOPAC93-PM3, Fujitsu, Tokyo, **1993**.
- ¹⁸ See Chapter 3 and references therein.
- ¹⁹ N. Koumura, R.W.J. Zijlstra, R.A. van Delden, N. Harada, B.L. Feringa, *Nature* **1999**, 401, 152.